

文章编号: 1005-6661(2021)02-0177-08 DOI: 10.16250/j.32.1374.2020317

·论著·

# PD-1/PD-L1在弓形虫感染小鼠妊娠中晚期的表达及与IFN-γ的相互调节作用

薛飒, 曾雨露, 闭香连, 卢韵宇, 张大义, 张立林, 韩雪, 杨军, 傅晓茵\*, 刘登宇\*

**[摘要]** 目的 探讨程序性死亡蛋白(programmed death protein-1, PD-1)及其配体PD-L1在小鼠妊娠早期弓形虫感染后母胎界面的动态表达, 及其与 $\gamma$ 干扰素(interferon- $\gamma$ , IFN- $\gamma$ )的相互调节作用。方法 将20只孕0 d母鼠随机平均分为4组, 即孕12 d对照组(12 dpn组)、孕12 d感染组(12 dpi组)和孕18 d对照组(18 dpn组)、感染组(18 dpi组)。在妊娠第6天时对12 dpi组、18 dpi组孕鼠给予150个弓形虫PRU株速殖子腹腔注射, 12 dpn组、18 dpn组孕鼠则注射等量PBS。于小鼠妊娠第12天和第18天分别处死4组小鼠, 计数胎盘、胎儿数量并称重。取各组孕鼠胎盘和子宫组织观察其组织病理变化, 采用实时荧光定量聚合酶链反应(qPCR)检测胎盘、子宫组织中PD-1与PD-L1、弓形虫表面抗原SAG-1及细胞因子IFN- $\gamma$  mRNA表达水平, 并分析PD-1与IFN- $\gamma$ 表达的相关性。设置12 dpn、12 dpi、18 dpn、18 dpi组以及12 dpi PBS阴性对照组、18 dpi PBS阴性对照组, 采用免疫组织化学染色检测孕鼠子宫、胎盘组织中PD-1表达水平。结果 12 dpi组和18 dpi组孕鼠均出现胎盘和胎儿发育不良等不良妊娠结局, 且胎盘重量和胎儿体质量均低于12 dpn组、18 dpn组( $t = 5.52, 11.44, 12.63, 11.67, P < 0.01$ )。组织病理观察结果显示, 12 dpi组和18 dpi组孕鼠胎盘组织蜕膜及连接区连接疏松, 胎盘及子宫组织中均见大量炎性细胞浸润和淤血。经qPCR检测发现, 12 dpn、12 dpi、18 dpn组和18 dpi组小鼠胎盘和子宫组织中PD-1、PD-L1、IFN- $\gamma$ 和SAG-1表达均存在差异( $F = 22.48, 51.23, 9.61, 47.49, 16.08, 21.52, 28.66, 238.90, P < 0.05$ ), 其中12 dpi组小鼠胎盘( $P < 0.05$ )及子宫组织中( $P < 0.05$ )中PD-1、PD-L1、IFN- $\gamma$ 和SAG-1表达水平均较12 dpn组升高。与18 dpn组相比, 18 dpi组小鼠胎盘组织中PD-1和PD-L1表达水平均下降( $P < 0.05$ ), 胎盘和子宫组织中IFN- $\gamma$ 和SAG-1表达水平均升高( $P < 0.05$ )。与12 dpi组相比, 18 dpi组孕鼠胎盘和子宫中PD-1和PD-L1表达水平均下降( $P < 0.05$ )。免疫组化染色结果显示, PD-1在12 dpi组孕鼠胎盘组织中浸润的炎性细胞上有表达, 在18 dpi组中表达不明显; PD-1在12 dpi组孕鼠子宫上皮呈强阳性表达, 而在18 dpi组呈弱阳性表达。相关分析结果显示, 12 dpi组孕鼠胎盘( $r_s = 0.99, P < 0.01$ )、子宫( $r_s = 0.97, P < 0.01$ ), 18 dpi组孕鼠胎盘( $r_s = 0.82, P < 0.05$ )、子宫( $r_s = 0.81, P < 0.05$ )中IFN- $\gamma$ 与PD-1 mRNA表达水平均呈正相关。**结论** 小鼠妊娠早期感染弓形虫后, 胎盘和子宫中PD-1/PD-L1表达呈孕中期显著上升、孕晚期下降的动态变化, 且与同期IFN- $\gamma$ 表达趋势一致, 其中PD-1与IFN- $\gamma$ 表达呈正相关; 故推测在孕鼠妊娠中、晚期, 母胎界面PD-1/PD-L1通路与弓形虫感染所诱导的IFN- $\gamma$ 有相互调节关系。

**[关键词]** 刚地弓形虫; 妊娠; 小鼠; PD-1/PD-L1;  $\gamma$ 干扰素

**[中图分类号]** R382.5 **[文献标识码]** A

## PD-1/PD-L1 expression and its interaction with interferon- $\gamma$ in *Toxoplasma gondii*-infected mice at middle and late pregnancy

XUE Sa, ZENG Yu-Lu, BI Xiang-Lian, LU Yun-Yu, ZHANG Da-Yi, ZHANG Li-Lin, HAN Xue, YANG Jun, FU Xiao-Yin\*, LIU Deng-Yu\*

Department of Parasitology, School of Preclinical Medicine, Guangxi Medical University, Nanning 530021, Guangxi Zhuang Autonomous Region, China

\* Corresponding authors

**[Abstract]** **Objective** To explore the dynamic expression of programmed cell death-1 (PD-1) and its ligand PD-L1 at the maternal-fetal interface of mice post-infection with *Toxoplasma gondii* at early pregnancy and examine its interaction with interferon-

**[基金项目]** 国家自然科学基金(81760370); 广西自然科学基金(2017GXNSFBA198154)

**[作者单位]** 广西医科大学基础医学院寄生虫学教研室(南宁530021)

**[作者简介]** 薛飒, 女, 硕士研究生。研究方向: 病原生物学

\* 通信作者 E-mail: fuxyin@outlook.com, ORCID: 0000-0002-9535-9299;  
E-mail: liudengyu@tom.com, ORCID: 0000-0002-8245-9573

**[数字出版日期]** 2021-04-16 08:41:31

**[数字出版网址]** <https://kns.cnki.net/kcms/detail/32.1374.R.20210415.1656.005.html>

$\gamma$  (IFN- $\gamma$ ). **Methods** A total of 20 mice at day 0 of pregnancy were randomly assigned into 4 groups, including the 12-day pregnancy control group (12 dpn group), 12-day pregnancy and infection group (12 dpi group), 18-day pregnancy control group (18 dpn group) and 18-day pregnancy and infection group (18 dpi group), respectively. On the 6th day of the pregnancy, mice in the 12 dpi and 18 dpi groups were injected intraperitoneally with 150 tachyzoites of the *T. gondii* PRU strain, while mice in the 12 dpn and 18 dpn groups were injected with the same volume of PBS. All mice in the four groups were sacrificed on 12th and 18th day of the pregnancy, and the number of placenta and fetus was counted and the weight of placenta and fetus was measured. Then, the placental and uterine tissues of the pregnant mice in each group were sampled for pathological examinations. The mRNA expression of *PD-1*, *PD-L1*, *T. gondii* surface antigen *SAG-1* and *IFN-γ* genes was quantified using a quantitative real-time PCR (qPCR) assay, and the correlation between *PD-1* and *IFN-γ* expression was examined. In addition, the 12 dpn group, 12 dpi group, 18 dpn group, 18 dpi group, PBS negative control of the 12 dpi group and PBS negative control of the 18 dpi group were assigned, and the *PD-1* expression was determined in the uterine and placenta tissues of the pregnant mice. **Results** Adverse pregnant outcomes were seen in mice in the 12 dpi and 18 dpi groups, including placental dysplasia and fetal maldevelopment, and the placental weights and fetal body weights were significantly lower in mice in the 12 dpi and 18 dpi groups than those in the 12 dpn and 18 dpn groups ( $t = 5.52, 11.44, 12.63$  and  $11.67$ , all  $P < 0.01$ ). The histopathological examinations showed that the decidua and junctional regions of the placental tissues were loosely connected in the 12 dpi and 18 dpi groups, and a large number of inflammatory cells infiltration and congestion were seen in the placental and uterine tissues. qPCR assay detected significant differences in *PD-1*, *PD-L1*, *IFN-γ* and *SAG-1* expression in the placental and uterine tissues among the 12 dpn, 12 dpi, 18 dpn and 18 dpi groups ( $F = 22.48, 51.23, 9.61, 47.49, 16.08, 21.52, 28.66$  and  $238.90$ , all  $P < 0.05$ ), and the *PD-1*, *PD-L1*, *IFN-γ* and *SAG-1* expression was all significantly higher in the placental and uterine tissues of mice in the 12 dpi group than in the 12 dpn group (all  $P$  values  $< 0.05$ ). The *PD-1* and *PD-L1* expression was significantly lower in the placental tissues of mice in the 18 dpi group than in the 18 dpn group (all  $P$  values  $< 0.05$ ), and the *IFN-γ* and *SAG-1* expression was significantly higher in the placental and uterine tissues of mice in the 18 dpi group than in the 18 dpn group (all  $P$  values  $< 0.05$ ), while the *PD-1* and *PD-L1* expression was significantly lower in the placental and uterine tissues of mice in the 18 dpi group than in the 12 dpi group (all  $P$  values  $< 0.05$ ). Immunohistochemical staining showed PD-1 expression in the inflammatory cells of the placental tissues of mice in the 12 dpi group, and no apparent PD-1 expression in the 18 dpi group, while strongly positive PD-1 expression was found in the uterine epithelium of mice in the 12 dpi group, and mildly strong expression was in the 18 dpi group. In addition, the *IFN-γ* mRNA expression was positively correlated with the *PD-1* mRNA expression in placental ( $r_s = 0.99, P < 0.01$ ) and uterine tissues of mice in the 12 dpi group ( $r_s = 0.97, P < 0.01$ ) and in placental ( $r_s = 0.82, P < 0.01$ ) and uterine tissues of mice in the 18 dpi group ( $r_s = 0.81, P < 0.01$ ). **Conclusions** Following *T. gondii* infection at early pregnancy, the *PD-1* and *PD-L1* expression shows a remarkable rise at middle pregnancy and a reduction at late pregnancy in placental and uterine tissues of mice, which appears the same tendency with *IFN-γ* expression during the same time period, and *PD-1* expression positively correlates with *IFN-γ* expression. The dynamic expression of PD-1 and PD-L1 on the maternal-fetal interface of mice may be mutually mediated by IFN- $\gamma$  induced by *T. gondii* infection.

**[Keywords]** *Toxoplasma gondii*; Pregnancy; Mice; PD-1/PD-L1; Interferon- $\gamma$

妊娠期间弓形虫感染可导致孕妇流产、死胎和先天性弓形虫病等不良妊娠结局<sup>[1]</sup>。在急性弓形虫感染情况下,出生婴儿可出现黄疸、发育迟缓、畸形、精神分裂、双侧性脉络膜视网膜炎等临床症状<sup>[1-2]</sup>。由弓形虫感染引起的母胎免疫调节尚未阐明。在妊娠期间,蜕膜基质细胞和胎盘滋养细胞等蜕膜非免疫细胞以及Th1和Th2型细胞、Th17细胞、调节性T细胞(Tregs)、子宫自然杀伤细胞等蜕膜免疫细胞,及其分泌的某些细胞因子间的相互作用对免疫平衡调节至关重要,而免疫抑制分子与这些蜕膜细胞的分化密切相关<sup>[3-5]</sup>。

程序性死亡蛋白(programmed death protein-1, PD-

1)作为免疫球蛋白超家族的负性调节因子,通过与其配体PD-L1/PD-L2结合来发挥免疫调节功能<sup>[6]</sup>。妊娠早期PD-1/PD-L1信号通路激活有助于营造母胎界面的免疫耐受微环境,有利于胚胎着床和发育<sup>[7]</sup>。研究发现,弓形虫感染孕鼠可出现母胎界面PD-1<sup>+</sup>和CTLA-4<sup>+</sup> Tregs细胞数量减少,但Tregs细胞上PD-1和CTLA-4表达量却高于正常妊娠小鼠,TGF-β可上调PD-1<sup>+</sup>和CTLA-4<sup>+</sup> Tregs细胞数量而改善妊娠结局<sup>[8-9]</sup>;母体分泌的雌二醇(E2)同样能通过促进Tregs细胞表达PD-1来减少细胞凋亡<sup>[10]</sup>。此外,在小鼠妊娠中期时,相对于外周血,母胎界面蜕膜NK细胞(uNK)表面PD-1表达量增加,而细胞毒性下降<sup>[11]</sup>。可见,PD-1/

PD-L1通路在母胎界面发挥重要作用。

$\gamma$ 干抗素(interferon- $\gamma$ , IFN- $\gamma$ )是宿主抵抗弓形虫感染的主要细胞因子,其水平上升可同步激活免疫细胞上PD-1表达。在肿瘤免疫机制中,IFN- $\gamma$ 可通过与其受体结合来激活JAK/STAT通路,以此来上调PD-1/PD-L1通路表达<sup>[12-13]</sup>。而当T细胞表面PD-1分子高度上调时,IFN- $\gamma$ 的表达又可因T细胞衰竭而下调<sup>[14]</sup>。另有研究发现,与PD-1同为负性免疫调节分子的TIM-3分子在弓形虫感染妊娠模型中与IFN- $\gamma$ 呈正向相关性表达<sup>[15]</sup>。由此可见,免疫抑制分子表达与IFN- $\gamma$ 调节作用密不可分,在妊娠期弓形虫感染中,PD-1可能参与宿主IFN- $\gamma$ 表达的负向调控,与妊娠结局有一定相关性。但孕期不同阶段PD-1/PD-L1动态表达情况尚未见相关报道,本研究探讨了PD-1分子在妊娠早期弓形虫感染后母胎界面的表达和调控作用。

## 材料与方法

### 1 动物与虫株来源

SPF级雌性昆明小鼠(7周龄)、雌性C57BL/6小鼠(7周龄)、雄性C57BL/6小鼠(8周龄)购于广西医科大学动物实验中心[动物生产或使用许可证号:SYXK(桂)2014-0003],在标准环境下饲养。刚地弓形虫PRU虫株由山东大学医学形态学教学实验室周怀瑜教授惠赠,经昆明小鼠传代。本研究获广西医科大学动物伦理委员会批准(批准号:201911010)。

### 2 主要试剂

伊红染液、Cole氏苏木素染液、Mayer'苏木素染液购自北京索莱宝科技有限公司;兔SP试剂盒购自北京中杉金桥生物科技有限公司;兔来源PD-1单克隆抗体购自英国Abcam公司;StarscriptII除基因组

cDNA第一链合成预混试剂、TRIGene总RNA提取剂、荧光定量PCR荧光染料SYBR购自日本TaKaRa公司。

### 3 弓形虫妊娠小鼠模型的建立

实验当晚19:00,按1:2的比例将8周龄雄性C57BL/6小鼠与7周龄雌性C57BL/6小鼠合笼,次日早上7:00检查雌性小鼠阴道口是否有白色阴栓,将有白色阴栓者记为孕0 d。将20只孕鼠随机分配到孕12 d对照组(12 dpn)、孕12 d感染组(12 dpi)和孕18 d对照组(18 dpn)、孕18 d感染组(18 dpi)4组中,每组5只孕鼠。12 dpi、18 dpi组孕鼠均在孕6 d时腹腔注射150个弓形虫PRU株速殖子,12 dpn组、18 dpn组注射相同体积PBS。妊娠第12天时处死12 dpi、12 dpn组孕鼠,妊娠第18天时处死18 dpi、18 dpn组孕鼠,取孕鼠子宫和胎盘组织用于后续检测。

### 4 胎盘和子宫组织切片及染色镜检

取各组小鼠胎盘和子宫组织,置于10%甲醛中性固定液中固定24 h用于石蜡包埋切片,经HE染色后显微镜下观察胎盘和子宫组织病理性改变;经免疫组化染色后观察PD-1在胎盘和子宫组织中的表达情况。免疫组化中为验证一抗的可靠性,加设12 dpi PBS阴性对照组和18 dpi PBS阴性对照组,即另取12 dpi组和18 dpi组小鼠组织,在进行一抗孵育时采用PBS代替一抗孵育过夜,其余操作步骤相同。免疫组化染色后,胞质内有棕色颗粒背景的细胞为PD-1表达阳性细胞。

### 5 实时荧光定量聚合酶链反应(qPCR)检测

根据产品说明书,以 $\beta$ -actin为内参,引物由生工生物工程上海股份有限公司合成,引物序列见表1。10  $\mu$ L反应体系包括SYBR荧光染料5  $\mu$ L,上、下游引物各0.5  $\mu$ L,cDNA 1  $\mu$ L、无菌去离子水3  $\mu$ L。使用荧

表1 qPCR反应引物序列  
Table 1 Sequence of primers used for the qPCR assay

引物 Primers	序列(5'→3') Sequence (5'→3')	参考文献 Reference
PD-1-F	GTGGCTGGAAATGGAGAT	[16]
PD-1-R	TAGGTGCTGGGCCATAGTA	
PD-L1-F	CGTCCTCAGTCAAGAGGAG	[16]
PD-L1-R	GTCCTAGAAGTGCCCAACA	
SAG1-F	CTGTCAGTTGCTGCGGAAGGAC	[17]
SAG1-R	CGTTAGCGTGGCACCATATTCACTC	
IFN- $\gamma$ -F	GGAACTGGCAAAGGATGGTGCAC	[17]
IFN- $\gamma$ -R	GCTGGACCTGTGGTTGTTGGAC	
$\beta$ -actin-F	TGGAATCCTGTGGCATCCATGAAAC	[17]
$\beta$ -actin-R	TAAAACGCAGCTCAGTAACAGTCCG	

光定量PCR仪,用两步法进行定量PCR扩增。反应条件如下:95℃ 30 s(预变性);95℃ 5 s,60℃ 30 s,进行40个循环扩增;95℃,65~95℃ 0.1℃/s(溶解曲线)。实验数据采用 $2^{-\Delta\Delta Ct}$ 方法进行分析。

## 6 统计分析

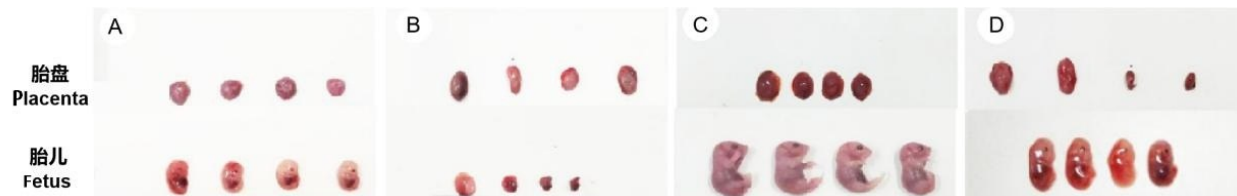
采用SPSS 23.0软件进行统计分析。计量资料多组间差异比较采用单因素方差分析,方差齐时组间两两比较采用LSD法检验,方差不齐时采用近似F检验Welch法;两组间差异比较采用两独立样本t检验,相

关性分析采用Spearman相关分析, $P < 0.05$ 为差异有统计学意义。

## 结 果

### 1 弓形虫感染后孕鼠胎儿和胎盘一般情况

12 dpn组和18 dpn组小鼠胎儿(图1A、C)发育良好,胎盘血供充足、大小均一;与上述同期对照组小鼠相比,12 dpi组和18 dpi组则出现明显胎盘缺血和胎儿发育不良,并有流产、死胎和胎儿减少(图1B、D)。



注:A 12 dpn组;B 12 dpi组;C 18 dpn组;D 18 dpi组。

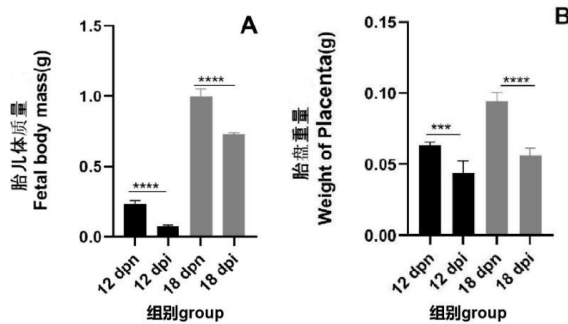
Note: A The 12 dpn group; B The 12 dpi group; C The 18 dpn group; D The 18 dpi group.

图1 感染组和对照组小鼠妊娠结局

Fig. 1 Pregnant outcomes of mice in the *Toxoplasma gondii* infection and control groups

### 2 弓形虫感染对孕鼠胎盘重量和胎儿体质量的影响

分别测量感染组和对照组每只孕鼠单个胎盘重量和胎儿体质量,结果显示,12 dpn组孕鼠胎儿平均体质量为 $(0.231 \pm 0.029)$  g,12 dpi组为 $(0.076 \pm 0.009)$  g,差异有统计学意义( $t = 12.63, P < 0.01$ );18 dpn组孕鼠胎儿平均体质量为 $(0.999 \pm 0.551)$  g,18 dpi组为 $(0.731 \pm 0.011)$  g,差异有统计学意义( $t = 11.67, P < 0.01$ )(图2A)。12 dpn组、12 dpi组孕鼠胎盘平均重量分别为 $(0.063 \pm 0.002)$ 、 $(0.046 \pm 0.005)$  g,差异有统计学意义( $t = 5.52, P < 0.01$ );18 dpn组、18 dpi组孕鼠胎盘平均重量为 $(0.094 \pm 0.006)$ 、 $(0.056 \pm 0.005)$  g,差异有统计学意义( $t = 11.44, P < 0.01$ )(图2B)。



注:A 各组胎儿体质量;B 各组胎盘重量。

Note: A Fetal body weight in each group; B Placenta weight in each group.

图2 各感染组和对照组孕鼠胎盘重量及胎儿体质量

Fig. 2 Placenta weight and fetal body weight of pregnant mice in the *Toxoplasma gondii* infection and control groups

### 3 孕鼠胎盘和子宫组织切片病理结果

显微镜下观察可见,12 dpn组和18 dpn组小鼠胎盘迷路细胞致密且排列整齐,迷路区血窦充血丰富(图3A、C)。12 dpi组小鼠胎盘迷路区细胞水肿,排列紊乱,血窦内血细胞减少(图3B);18 dpi组小鼠胎盘蜕膜及连接区出现明显纤维素样坏死,胎盘迷路区出现淤血、血窦扩张(图3D)。12 dpi组和18 dpi组小鼠子宫柱状上皮细胞均出现一定程度损伤,血管内血细胞数量减少,并有大量炎性细胞浸润(图3F、H)。

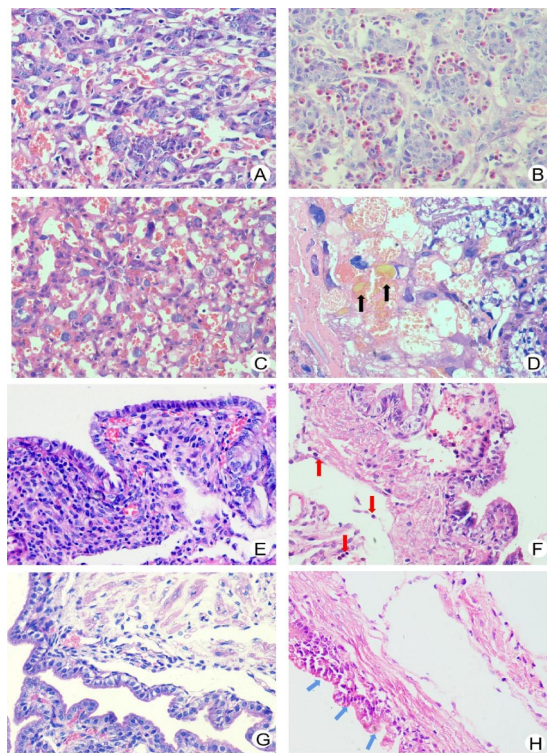
### 4 小鼠胎盘和子宫组织中PD-1表达

免疫组化染色结果显示,12 dpi PBS阴性对照组和18 dpi PBS阴性对照组小鼠胎盘以及子宫中均无PD-1阳性细胞(图4A、D、G、J),12 dpn组和18 dpn组小鼠胎盘及子宫组织中也未见PD-1阳性细胞(图4B、E、H、K)。12 dpi组小鼠胎盘组织中发现PD-1表达强阳性细胞(图4C),散在分布于胎盘组织中;油镜下对这些细胞进行细胞形态学观察,发现大多数为炎性细胞。18 dpi组小鼠胎盘组织未发现PD-1表达阳性细胞(图4F)。此外,PD-1在12 dpi组小鼠子宫黏膜柱状上皮细胞中呈强阳性表达(图4I),在18 dpi组小鼠子宫中呈弱阳性表达(图4L)。

### 5 PD-1、PD-L1、IFN-γ 和 SAG-1 在小鼠胎盘和子宫组织中表达水平

qPCR检测显示,12 dpn、12 dpi、18 dpn组和18

dpi 组小鼠胎盘和子宫组织中 *PD-1*、*PD-L1*、*IFN-γ*、*SAG-1* 表达存在差异 ( $F = 22.48, 51.23, 9.61, 47.49, 16.08, 21.52, 28.66, 238.90$ ,  $P$  均  $< 0.05$ )；与 12 dpi 组相比，12 dpi 组小鼠胎盘和子宫组织中 *PD-1*、*PD-L1* 和 *IFN-γ mRNA* 表达水平均上升 ( $P$  均  $< 0.05$ ) (图 5A、B、C、D、E、F)；而 18 dpi 组小鼠胎盘中 *PD-1* ( $P < 0.05$ ) 和 *PD-L1 mRNA* 表达水平 ( $P < 0.01$ ) 较 18 dpi 组显著下降 (图 5A、C)。18 dpi 组小鼠胎盘组织中 *PD-1 mRNA* 表达水平较 12 dpi 组上升 ( $P < 0.01$ )，18 dpi 组小鼠胎盘组织中 *PD-1 mRNA* 较 12 dpi 组表达下降 ( $P < 0.01$ ) (图 5A)。18 dpi 组小鼠胎盘组织中 *IFN-γ mRNA* 水平显著高于 18 dpi 组 ( $P < 0.05$ )，但低于 12 dpi 组 ( $P < 0.05$ ) (图 5E)。



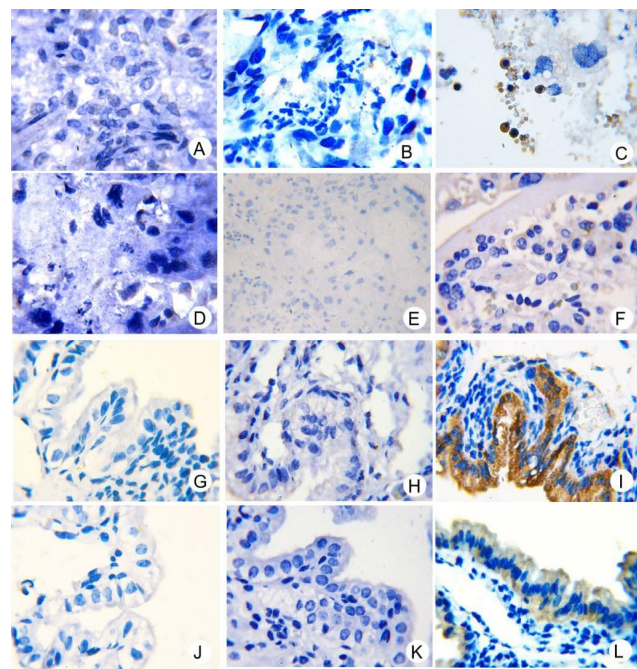
注：A、C 分别为 12 dpi 组和 18 dpi 组小鼠胎盘迷路区；图 B、D 分别为 12 dpi 组和 18 dpi 组小鼠胎盘迷路区(黑色箭头所示为淤血)；E、G 分别为 12 dpi 组和 18 dpi 组小鼠子宫组织；F、H 分别为 12 dpi 组和 18 dpi 组小鼠子宫组织(蓝色箭头所示为柱状上皮损伤，红色箭头所示为炎性细胞浸润)。

Note: A and C The mouse placental labyrinth areas in the 12 dpi and 18 dpi groups; B and D The mouse placental labyrinth areas in the 12 dpi and 18 dpi groups (the black arrows show the congestion); E and G Mouse uterine tissues in the 12 dpi and 18 dpi groups; F and H Mouse uterine tissues in the 12 dpi and 18 dpi groups (the blue arrows indicate the columnar epithelial injury, and the red arrows indicate the inflammatory cell infiltration).

**图3 各组小鼠胎盘及子宫组织病理改变(HE染色, ×400)**

**Fig. 3 Pathological changes of mouse placenta and uterine tissues in each group (HE staining,  $\times 400$ )**

小鼠胎盘和子宫组织中 *SAG-1 mRNA* 水平均显著上调，并在 12 dpi 组 ( $P < 0.01$ ) 上调最明显(图 5G、H)。



注：A ~ C 12 dpi PBS 阴性对照组、12 dpi 组、12 dpi 组小鼠胎盘迷路区；D ~ F 18 dpi PBS 阴性对照组、18 dpi 组、18 dpi 组小鼠胎盘迷路区；G ~ I 12 dpi PBS 阴性对照组、12 dpi 组、12 dpi 组小鼠子宫柱状上皮；J ~ L 18 dpi PBS 阴性对照组、18 dpi 组和 18 dpi 组小鼠子宫柱状上皮。

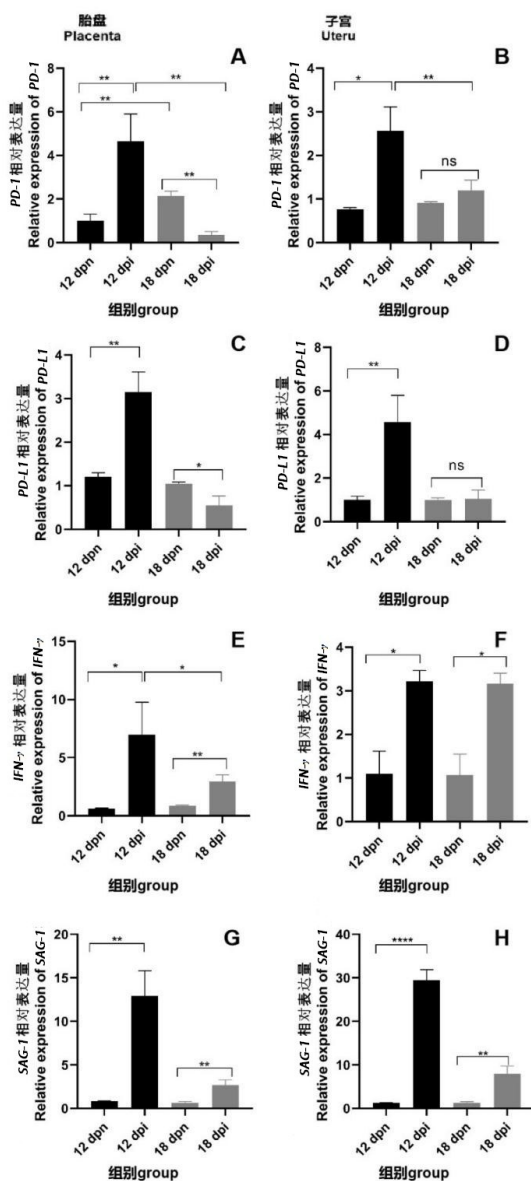
Note: A, B and C Placental labyrinth areas of mice in the PBS negative control group of the 12 dpi group, the 12 dpi group and the 12 dpi group; D, E and F Placental labyrinth areas of mice in the PBS negative control group of the 18 dpi group, the 18 dpi group and the 18 dpi group; G, H and I Uterine columnar epithelium of mice in the PBS negative control group of the 12 dpi group, 12 dpi group and the 12 dpi group; J, K and L Uterine columnar epithelium of mice in the PBS negative control group of the 18 dpi group, 18 dpi group and the 18 dpi group.

**图4 各组小鼠胎盘及子宫组织PD-1表达情况  
(IHC染色,  $\times 1000$ )**

**Fig. 4 PD-1 expression in mouse placenta and uterine tissues in each group (IHC staining,  $\times 1000$ )**

## 6 弓形虫感染组小鼠胎盘、子宫中 *IFN-γ* 与 *PD-1* 表达相关性

12 dpi 组小鼠胎盘 ( $r_s = 0.99, P < 0.01$ , 图 6A)、子宫 ( $r_s = 0.97, P < 0.01$ , 图 6B), 18 dpi 组小鼠胎盘 ( $r_s = 0.82, P < 0.05$ , 图 6C)、子宫 ( $r_s = 0.81, P < 0.05$ , 图 6D) 中 *IFN-γ mRNA* 与 *PD-1 mRNA* 表达水平均呈正相关。

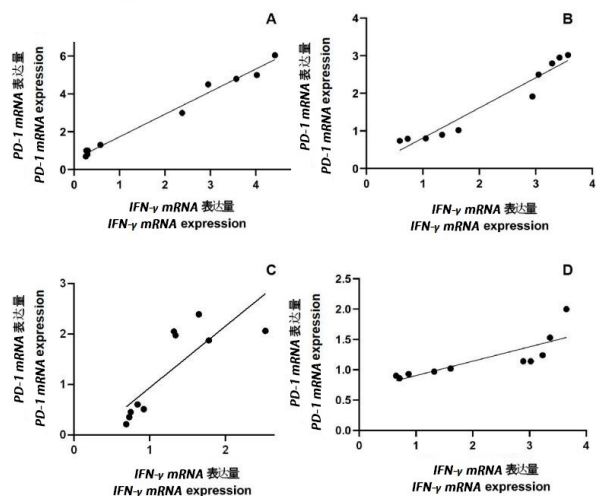


注: A 胎盘中 *PD-1* 基因相对表达量; B 子宫中 *PD-1* 基因相对表达量; C 胎盘中 *PD-L1* 基因相对表达量; D 子宫中 *PD-L1* 基因相对表达量; E 胎盘中 *IFN-γ* 基因相对表达量; F 子宫中 *IFN-γ* 基因相对表达量; G 胎盘中 *SAG-1* 基因相对表达量; H 子宫中 *SAG-1* 基因相对表达量。\*  $P < 0.05$ ; \*\*  $P < 0.01$ ; \*\*\*\*  $P < 0.0001$ ; ns  $P > 0.05$ 。

Note: A The relative expression of *PD-1* in the placenta; B The relative expression of *PD-1* in the uterus; C The relative expression of *PD-L1* in the placenta; D The relative expression of *PD-L1* in the uterus; E The relative expression of *IFN-γ* in the placenta; F The relative expression of *IFN-γ* in the uterus; G The relative expression of *SAG-1* in the placenta; H The relative expression of *SAG-1* in the uterus. \*  $P < 0.05$ ; \*\*  $P < 0.01$ ; \*\*\*\*  $P < 0.0001$ ; ns  $P > 0.05$ .

**图5 各组小鼠胎盘、子宫中 *PD-1*、*PD-L1*、*IFN-γ* 和 *SAG-1* 基因表达**

**Fig. 5 Expression of *PD-1*, *PD-L1*, *IFN-γ* and *SAG-1* in mouse placenta and uterine tissues in each group**



注: A 12 dpi 组胎盘; B 12 dpi 组子宫; C 18 dpi 组胎盘中; D 18 dpi 组子宫。

Note: A Mouse placenta in the 12 dpi group; B Mouse uterus in the 12 dpi group; C Mouse placenta in the 18 dpi group; D Mouse uterus in the 18 dpi group.

## 图6 感染小鼠胎盘、子宫中 *IFN-γ* 与 *PD-1* 表达的相关性

**Fig. 6 Correlation between *IFN-γ* and *PD-1* expression in the placenta and uterus of *Toxoplasma gondii*-infected mice**

## 讨 论

据报道,2001年全球孕妇急性弓形虫感染总体患病率为1.1%;弓形虫速殖子可经胎盘垂直传播给胎儿,导致流产及胎儿先天性弓形虫病<sup>[18]</sup>。孕早期发生弓形虫急性感染后,虫体自身毒力蛋白可通过影响子宫蜕膜化进程而导致不良妊娠结局;除此以外,由弓形虫感染引起的母胎界面强烈的炎性反应对胎儿造成致命的免疫病理损伤也是关注焦点之一<sup>[10, 19]</sup>。弓形虫感染发生在不同妊娠阶段可导致不同妊娠结局。研究表明,用 $5 \times 10^4$ 个弓形虫RH株速殖子分别感染妊娠早期和晚期C57BL/6小鼠,感染3 d后,仅早期感染孕鼠出现明显不良妊娠结局<sup>[10]</sup>。而另一项研究发现,在妊娠11 d时用30个Fukaya株包囊感染C57BL/6孕鼠,一周后在孕鼠胎盘组织发现大量虫体和明显的炎性细胞浸润<sup>[20]</sup>。以上研究表明,不同感染时期及不同虫株弓形虫感染对妊娠结局影响不同。本研究在C57BL/6小鼠早期妊娠第6天时对其给予腹腔注射150个弓形虫PRU株速殖子,发现感染后孕中期和孕晚期小鼠均出现流产、胎儿体质量和胎盘重量显著降低等情况;组织切片镜检发现,12 dpi组和18 dpi组孕鼠胎盘蜕膜区和子宫组织出现大量炎性细胞浸润、淤血等病理改变,提示妊娠早期弓形虫PRU株速殖子感染可导致孕中期和孕晚期出现不良妊娠结局。

*IFN-γ* 主要由抗原特异杀伤性 CD8<sup>+</sup>T 细胞产生,

通过IFN- $\gamma$ 诱导所产生的一氧化氮合酶等物质可抑制弓形虫生长并直接杀伤虫体<sup>[21]</sup>。由于IFN- $\gamma$ 有终止妊娠的作用,因此在正常妊娠的母胎界面几乎检测不到其表达<sup>[22]</sup>。本研究观察到,12 dpi组和18 dpi组小鼠子宫和胎盘中IFN- $\gamma$ 表达水平均显著升高,且孕12 d时表达量高于孕18 d;SAG1表达水平在12 dpi组和18 dpi组孕鼠子宫和胎盘中均有升高,且在孕12 d升高最为明显。此结果提示,当发生孕早期弓形虫感染后,孕中期母胎界面虫体载量最大,由此引发母胎界面强烈的炎症反应,并刺激免疫细胞分泌IFN- $\gamma$ 。

PD-1是可通过诱导T细胞衰竭而下调IFN- $\gamma$ 表达的负性调控分子<sup>[14]</sup>,但有关其在患妊娠相关疾病孕妇体内表达情况的研究结果不尽相同:Li等<sup>[23]</sup>发现在早期复发性流产孕妇体内,PD-1表达与正常妊娠孕妇无明显差异,但其配体PD-L1表达量下降,提示早期复发性流产与PD-1无相关性,而与PD-L1密切相关;但Xu等<sup>[24]</sup>研究却发现,PD-1和PD-L1在复发性流产发生时均表达下降。在子痫的疾病过程中,PD-1/PD-L1通路表达下调可导致Treg和Th17细胞比例下调,从而引发不良妊娠结局<sup>[25]</sup>。亦有研究发现,在临幊上使用抗CTLA-4和PD-1制剂治疗可促进患黑色素瘤的产妇顺利生产<sup>[26]</sup>。在孕鼠感染弓形虫的疾病模型中,孕早期和孕晚期分别用弓形虫RH株速殖子感染孕鼠,3 d后发现各感染组孕鼠胎盘中PD-1表达水平均上调<sup>[10]</sup>。以上提示在不同妊娠疾病模型中,PD-1/PD-L1通路表达有所差异。为了解孕早期弓形虫感染后PD-1/PD-L1在母胎界面中各时间点的表达情况,本研究检测了小鼠妊娠中、晚期PD-1/PD-L1的表达水平。结果提示,在正常妊娠状态下,孕18 d小鼠胎盘和子宫组织中PD-1表达水平随孕期延长呈上升趋势;而感染状态下,孕12 d时小鼠胎盘和子宫中PD-1和PD-L1表达水平均较对照组显著上升,孕18 d时PD-1和PD-L1表达则较同期对照组显著下降,且后者PD-1和PD-L1表达均较前者显著下降。对PD-1进行免疫组化染色观察发现,12 dpi组孕鼠胎盘和子宫组织中PD-1呈强阳性表达,而18 dpi组胎盘组织中不表达PD-1,其子宫组织中PD-1呈弱阳性表达,此表达趋势与PCR检测结果基本一致。另外,本研究同时对感染弓形虫孕鼠胎盘和子宫中PD-1与IFN- $\gamma$ 的表达进行了相关分析,发现两者表达呈正相关。故我们推测,在孕12 d感染阶段,由于机体识别弓形虫抗原而触发Th1型细胞免疫,并分泌IFN- $\gamma$ 等细胞因子,同步激活了免疫细胞上PD-1/PD-L1的表达<sup>[27]</sup>;而PD-1作为免疫负调控分子,又可诱导T细胞的衰竭,因此

在孕18 d时IFN- $\gamma$ 的表达较孕12 d明显下调。

本研究通过腹腔注射方式建立了C57BL/6小鼠妊娠早期弓形虫急性感染模型,首次连续观察了孕早期发生弓形虫感染后,孕鼠在孕中、晚期时母胎界面PD-1/PDL-1表达的动态波动情况,并分析了其与IFN- $\gamma$ 表达的相关性,为PD-1/PD-L1作为免疫靶标用于治疗先天性弓形虫病提供了实验基础和理论依据。

## 【参考文献】

- [1] Hampton MM. Congenital toxoplasmosis: a review [J]. Neonatal Netw, 2015, 34(5): 274-278.
- [2] Higa LT, Araújo SM, Tsuneto L, et al. A prospective study of *Toxoplasma*-positive pregnant women in southern Brazil: a health alert [J]. Trans R Soc Trop Med Hyg, 2010, 104(6): 400-405.
- [3] Ishida Y, Agata Y, Shibahara K, et al. Induced expression of PD-1, a novel member of the immunoglobulin gene superfamily, upon programmed cell death[J]. EMBO J, 1992, 11(11): 3887-3895.
- [4] Lash GE, Schiessl B, Kirkley M, et al. Expression of angiogenic growth factors by uterine natural killer cells during early pregnancy [J]. J Leukoc Biol, 2006, 80(3): 572-580.
- [5] Liu W, Luo M, Zou L, et al. uNK cell-derived TGF- $\beta$ 1 regulates the long noncoding RNA MEG3 to control vascular smooth muscle cell migration and apoptosis in spiral artery remodeling [J]. J Cell Biochem, 2019, 120(9): 15997-16007.
- [6] Robson A, Harris LK, Innes BA, et al. Uterine natural killer cells initiate spiral artery remodeling in human pregnancy [J]. FASEB J, 2012, 26(12): 4876-4885.
- [7] Zhang Y, Ma L, Hu X, et al. The role of the PD-1/PD-L1 axis in macrophage differentiation and function during pregnancy [J]. Hum Reprod, 2019, 34(1): 25-36.
- [8] Liu Y, Zhao M, Xu X, et al. Adoptive transfer of Treg cells counters adverse effects of *Toxoplasma gondii* infection on pregnancy [J]. J Infect Dis, 2014, 210(9): 1435-1443.
- [9] Zhao M, Zhang H, Liu X, et al. The effect of TGF- $\beta$  on Treg cells in adverse pregnancy outcome upon *Toxoplasma gondii* infection [J]. Front Microbiol, 2017, 8: 901.
- [10] Qiu J, Zhang R, Xie Y, et al. Estradiol attenuates the severity of primary *Toxoplasma gondii* infection-induced adverse pregnancy outcomes through the regulation of tregs in a dose-dependent manner [J]. Front Immunol, 2018, 9: 1102.
- [11] Jiang W, Deng Y, Song Z, et al. Gestational perfluorooctanoic acid exposure inhibits placental development by dysregulation of labyrinth vessels and uNK cells and apoptosis in mice [J]. Front Physiol, 2020, 11: 51.
- [12] Garcia-Diaz A, Shin DS, Moreno BH, et al. Interferon receptor signaling pathways regulating PD-L1 and PD-L2 expression [J]. Cell Rep, 2017, 19(6): 1189-1201.
- [13] Qian J, Wang C, Wang B, et al. The IFN- $\gamma$ /PD-L1 axis between T cells and tumor microenvironment: hints for glioma anti-PD-1/PD-L1 therapy [J]. J Neuroinflammation, 2018, 15(1): 290.
- [14] Ding G, Shen T, Yan C, et al. IFN- $\gamma$  down-regulates the PD-1 ex-

- pression and assist nivolumab in PD-1-blockade effect on CD8<sup>+</sup> T-lymphocytes in pancreatic cancer [J]. BMC Cancer, 2019, 19(1): 1053.
- [15] Fu X, Wu B, Huang B, et al. The correlation of Tim-3 and IFN- $\gamma$  expressions in mice infected with *Toxoplasma gondii* during gestation [J]. Parasitol Res, 2015, 114(1): 125-132.
- [16] Cao J, Liu FX, Yu MX. Expression of programmed death 1 and its ligands in the liver of autoimmune hepatitis C57BL/6 mice [J]. Chin Med J (Engl), 2009, 122(16): 1941-1946.
- [17] Jones LA, Roberts F, Nickdel MB, et al. IL-33 receptor (T1/ST2) signalling is necessary to prevent the development of encephalitis in mice infected with *Toxoplasma gondii* [J]. Eur J Immunol, 2010, 40(2): 426-436.
- [18] Bessières MH, Berrebi A, Rolland M, et al. Neonatal screening for congenital toxoplasmosis in a cohort of 165 women infected during pregnancy and influence of in utero treatment on the results of neonatal tests [J]. Eur J Obstet Gynecol Reprod Biol, 2001, 94(1): 37-45.
- [19] Sabou M, Doderer - Lang C, Leyer C, et al. *Toxoplasma gondii* ROP16 kinase silences the cyclin B1 gene promoter by hijacking host cell UHRF1-dependent epigenetic pathways [J]. Cell Mol Life Sci, 2020, 77(11): 2141-2156.
- [20] Shiono Y, Mun HS, He N, et al. Maternal - fetal transmission of *Toxoplasma gondii* in interferon - gamma deficient pregnant mice [J]. Parasitol Int, 2007, 56(2): 141-148.
- [21] Sasai M, Pradipta A, Yamamoto M. Host immune responses to *Toxoplasma gondii* [J]. Int Immunol, 2018, 30(3): 113-119.
- [22] Si LF, Zhang SY, Gao CS, et al. Effects of IFN- $\gamma$  on IL-18 expression in pregnant rats and pregnancy outcomes [J]. Asian-Australas J Anim Sci, 2013, 26(10): 1399-1405.
- [23] Li G, Lu C, Gao J, et al. Association between PD-1/PD-L1 and T regulate cells in early recurrent miscarriage [J]. Int J Clin Exp Pathol, 2015, 8(6): 6512-6518.
- [24] Xu YY, Wang SC, Lin YK, et al. Tim-3 and PD-1 regulate CD8(+) T cell function to maintain early pregnancy in mice [J]. J Reprod Dev, 2017, 63(3): 289-294.
- [25] Zhang Y, Liu Z, Tian M, et al. The altered PD-1/PD-L1 pathway delivers the ‘one-two Punch’ effects to promote the Treg/Th17 imbalance in pre-eclampsia [J]. Cell Mol Immunol, 2018, 15(7): 710-723.
- [26] Buecheit AD, Hardy JT, Szender JB, et al. Conception and viable twin pregnancy in a patient with metastatic melanoma while treated with CTLA-4 and PD-1 checkpoint inhibition [J]. Melanoma Res, 2020, 30(4): 423-425.
- [27] Sayama S, Nagamatsu T, Schust DJ, et al. Human decidual macrophages suppress IFN- $\gamma$  production by T cells through costimulatory B7-H1: PD-1 signaling in early pregnancy [J]. J Reprod Immunol, 2013, 100(2): 109-117.

【收稿日期】 2020-11-30 【编辑】 邓瑶

(上接第119页)

- [84] Nichols GL, Freedman J, Pollock KG, et al. *Cyclospora* infection linked to travel to Mexico, June to September 2015 [J]. Euro Surveill, 2015, 20(43): 30048.
- [85] Marques DFP, Alexander CL, Chalmers RM, et al. Cyclosporiasis in travellers returning to the United Kingdom from Mexico in summer 2017: lessons from the recent past to inform the future [J]. Euro Surveill, 2017, 22(32): 30592.
- [86] Li W, Feng Y, Santin M. Host specificity of *Enterocytozoon bieneusi* and public health implications [J]. Trends Parasitol, 2019, 35(6): 436-451.
- [87] Guo Y, Alderisio KA, Yang W, et al. Host specificity and source of *Enterocytozoon bieneusi* genotypes in a drinking source watershed [J]. Appl Environ Microbiol, 2014, 80(1): 218-225.
- [88] Didier ES, Weiss LM, Cali A, et al. Overview of the presentations on microsporidia and free-living amebae at the 10th International Workshops on Opportunistic Protists [J]. Eukaryot Cell, 2009, 8 (4): 441-445.
- [89] Gong B, Yang Y, Liu X, et al. First survey of *Enterocytozoon bieneusi* and dominant genotype Peru6 among ethnic minority groups in southwestern China’s Yunnan Province and assessment of risk factors [J]. PLoS Negl Trop Dis, 2019, 13(5): e0007356.
- [90] López-Vélez R, Turrientes M C, Garrón C, et al. Microsporidiosis in travelers with diarrhea from the tropics [J]. J Travel Med, 1999, 6(4): 223-227.
- [91] Müller A, Bialek R, Kämper A, et al. Detection of microsporidia in travelers with diarrhea [J]. J Clin Microbiol, 2001, 39(4): 1630-1632.
- [92] Wichro E, Hoelzl D, Krause R, et al. Microsporidiosis in travel-associated chronic diarrhea in immune-competent patients [J]. Am J Trop Med Hyg, 2005, 73(2): 285-287.
- [93] Bryant AS, Hallem EA. Terror in the dirt: Sensory determinants of host seeking in soil-transmitted mammalian-parasitic nematodes [J]. Int J Parasitol Drugs Drug Resist, 2018, 8(3): 496-510.
- [94] Brunet J, Lemoine JP, Lefebvre N, et al. Bloody diarrhea associated with hookworm infection in traveler returning to France from Myanmar [J]. Emerg Infect Dis, 2015, 21(10): 1878.
- [95] Wesołowska M, Rymer W, Kicia M, et al. Concurrent infection of a young tourist by hookworm and *Strongyloides stercoralis* during low budget travel in Southeast Asia [J]. Helminthologia, 2018, 55(2): 166-172.
- [96] Yoshikawa M, Ouchi Y, Hirai N, et al. *Ancylostoma ceylanicum*, novel etiological agent for traveler’s diarrhea—report of four Japanese patients who returned from Southeast Asia and Papua New Guinea [J]. Trop Med Health, 2018, 46: 6.
- [97] Prosl H. Holiday dreams with a downside: uncommon tapeworm infection in an infant [J]. Wien Klin Wochenschr, 2005, 117(4): 56-59.

【收稿日期】 2020-10-10 【编辑】 汪伟